Macromolecules

Article

Cite This: Macromolecules 2018, 51, 9156−9164

pubs.acs.org/Macromolecules

kT-Scale Interactions and Stability of Colloids with Adsorbed Zwitterionic and Ethylene Oxide Copolymers

Matthew G. Petroff,[†] Elena Alexandra Garcia,[†] Raymond A. Dengler,[†] Margarita Herrera-Alonso,*[,‡] and Michael A. Bevan*[,†]

[†]Chemical and Biomolecular Engineering, Johns Hopkins University, Baltimore, Maryland 21218, United States

[‡]Chemical and Biological Engineering, Colorado State University, Fort Collins, Colorado 80523, United States

Supporting Information

ABSTRACT: We report synthesis of novel zwitterionic triblock copolymers and direct measurements of their interactions when adsorbed to colloids and surfaces. We investigate triblock copolymers with poly(2-methacryloyloxyethylphosphorylcholine) (PMPC) end blocks separated by a poly(propylene oxide) (PPO) center block, with comparison to poly(ethylene oxide) PEO−PPO−PEO analogues. Interaction potentials are measured for a molecular weight series of PMPC and PEO copolymers adsorbed to hydrophobic colloids of varying diameter and planar surfaces. Findings indicate that, for the same number of repeat units, PMPC brushes generate repulsion at several times the distance of PEO brushes. PEO brush dimensions and interactions show good agreement with polymer brush models, whereas PMPC interactions suggest layer architectures with chain extensions approaching the PMPC block contour length. While PEO blocks must have 2−3 times as many repeat units to generate the same thickness as PMPC blocks, PMPC and PEO layers of the same thickness generate equivalent interactions and colloidal stability.

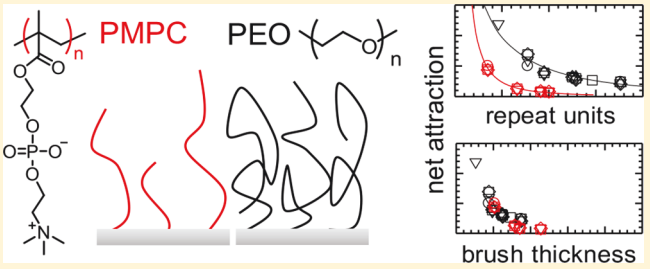

INTRODUCTION

Prevention of particle aggregation and deposition in physiological media is critical to applications involving biosensors,[1,2] drug delivery,[3] and filtration.[4] Adsorption of polymers to colloidal particles and surfaces is a common strategy to stabilize colloids against aggregation and prevent their deposition onto surfaces. Polymer layers that are effective at stabilizing colloidal particles against aggregation and deposition must generate repulsion of sufficient range and magnitude to overcome attractive interactions.[5] The range and magnitude of repulsion are enhanced for layers with "polymer brush" architectures, where lateral crowding causes chains to extend away from surfaces.[6] Polymer chemistries that have been found to be most favorable for generating repulsion are often well solvated and uncharged, presumably to minimize attractive segment interactions.[7−9] Poly(ethylene oxide) (PEO) satisfies many of the cited physical and chemical constraints and is widely considered as the benchmark for colloidal stabilization in physiological ionic strength aqueous media.[3,10−12]

Zwitterionic polymer chemistries have gained attention as potential alternatives to PEO.[13,14] Zwitterionic polymers are composed of a hydrocarbon backbone with zwitterionic moieties, which consist of positive and negative functional groups with a net neutral charge and significant dipole moments. Several studies have demonstrated zwitterionic polymer surface layers to reduce adhesion of proteins[15] and cells,[1] increase colloidal stability,[16] and increase drug circulation time.[17] Enhanced antifouling by zwitterionic polymers is often attributed to "superhydrophilicity" of zwitterionic polymers (i.e., favorable water−monomer interactions[14] inferred from simulations[13] and spectroscopy[18]). However, several conflicting studies have reported either equivalent[1,19−21] or inferior[20,22] colloidal stabilization and antifouling behavior by zwitterionic polymers relative to PEO. This suggests there is more to understand in the net interactions of zwitterionic and PEO copolymers.

Varied findings in comparative studies of zwitterionic and PEO polymers may partly arise from limitations on controlling or characterizing layer architectures. Many studies investigate either "grafted-to" layers, which often produce lower surface concentrations, or "grafted-from" layers, which are more difficult to characterize (since chains must be removed for analysis).[7,23] Another strategy is to use physisorbed copolymers, which are straightforward to process and characterize (prior to adsorption). First-principles design of copolymer compositions and architectures is not trivial based on a complex balance of segment, solvent, and surface interactions. However, copolymers capable of forming thick, dense layers via physisorption have been identified.[24,25] A notable example is PEO−PPO−PEO triblock copolymers, which are well established for stabilizing hydrophobic colloids in aqueous media.[11,25,26] While a number of studies have investigated the

Received: August 18, 2018
Revised: October 11, 2018
Published: November 7, 2018

DOI: 10.1021/acs.macromol.8b01792
Macromolecules 2018, 51, 9156−9164

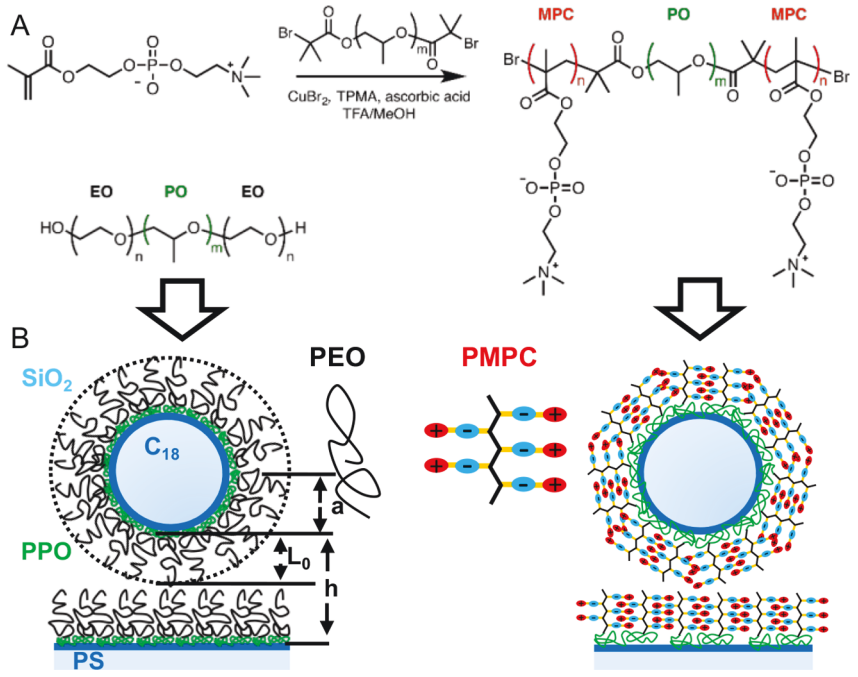

Figure 1. Synthesis of PMPC triblock copolymers and adsorption onto hydrophobic colloids and surfaces. (A) Synthesis of PMPC−PPO−PMPC by ARGET-ATRP from a PPO_{48} macroinitiator. (B) Configuration for adsorption and schematic architecture of commercial PEO−PPO−PEO and synthesized PMPC−PPO−PMPC on hydrophobically modified (silane) silica colloids and glass microscope slides. The sphere−wall geometry is used to measure interaction potentials and deposition behavior. PMPC and PEO triblock copolymer molecular weights and number of repeat units are reported in Tables S1 and S2.

phase behavior and emulsion stabilizing ability of zwitterionic copolymers,[27−30] less have explored their use as colloidal stabilizers.[31,32] Many studies have explored synthesis of novel polymers, but none have systematically studied connections between layer properties, interactions, or effects on colloidal aggregation and deposition.

Although interactions of zwitterionic and EO polymers determine all of their behaviors and properties, a limited number of studies have directly measured or modeled such interactions. Several studies have measured polymer layer interactions,[33−37] typically at high applied normal forces that produce significant compression. High normal forces and layer deformation are important to adhesion, friction, and lubrication between adsorbed layers but are less relevant to colloidal stability. Colloidal stability is determined by the net balance of competing colloidal interactions at the very onset of repulsion between adsorbed layers.[38−42] In particular, colloidal stabilization is highly sensitive to *kT*-scale repulsion between adsorbed polymer layers for weak interpenetration and compression of adsorbed layers at the periphery of the adsorbed layer architecture where their density profile vanishes.[6,39] The authors are unaware of measurements of zwitterionic copolymer interactions in the regimes relevant to colloidal stability. Furthermore, we are unaware of any systematic studies of how block chemistries, molecular weights, and adsorbed layer architectures are related to interactions critical to colloidal stability.

Here, we report measured interactions between PEO and zwitterionic copolymers adsorbed to hydrophobic colloids and surfaces. Measurement of symmetric interactions in this work provide a basis to understand colloidal stability and a basis for future measurements of asymmetric interactions with biomaterials relevant to antifouling coatings and drug delivery. Measurements are reported for commercial PEO−PPO−PEO copolymers as well as novel zwitterionic copolymers of PMPC−PPO−PMPC (Figure 1). Ensemble total internal reflection microscopy (TIRM)[43] is used to measure potential energy profiles with *kT* and nanometer scale resolution between adsorbed triblock copolymer layers with varying molecular weights of the PEO and PMPC end blocks. Additional characterization of adsorbed layers by dynamic light scattering and quartz-crystal microbalance in conjunction with theoretical models is used to compare and contrast PEO and PMPC copolymer layer properties, architecture, and interactions. Finally, measured interactions are connected to colloidal stability against deposition and aggregation for a range of colloid diameters and copolymer molecular weights. Our findings show important differences in PEO and PMPC copolymer interactions and architectures that determine colloidal stability in physiological media.

MATERIALS AND METHODS

PEO−PPO−PEO and PMPC−PPO−PMPC Copolymers. PEO−PPO−PEO copolymers were donated by BASF with details in Table S2. PMPC−PPO−PMPC triblock copolymers were synthesized by polymerization of MPC monomer onto Br-PPO_{48}−Br macroinitiator by activator regenerated by electron transfer-atom transfer radical polymerization (ARGET-ATRP) with copper catalyst. PPO_{48} macroinitiator (Br-PPO_{48}-Br) (50 mg, 0.016 mmol) and MPC (953 mg, 3.23 mmol, 100 mol equiv to -Br) were dissolved in methanol (3 mL). Tris(2-pyridylmethyl)amine (TPMA) ligand and ascorbic acid (reducing agent) were also prepared in methanol at 10 mg/mL each. Aliquots of the TPMA solution (187 μL, 6.5 μmol, 10 mol equiv to Cu) and ascorbic acid solutions (114 μL, 6.5 μmol, 10 mol equiv to Cu) were added to the flask that contained the macroinitiator and monomer, sealed, and bubbled with argon for 40 min at room temperature. Separately, a stock solution of $CuBr_2$ catalyst was prepared in methanol at 2 mg/mL and bubbled under nitrogen for 30 min. The flask containing macroinitiator, MPC, TMPA, and ascorbic

DOI: 10.1021/acs.macromol.8b01792
Macromolecules 2018, 51, 9156−9164

acid was immersed in an oil bath at 40 °C, and the reagents were homogenized under vigorous argon flow for ∼2 min. Polymerization was started by the addition of $CuBr_2$ solution (72 μL, 0.65 μmol, 200 ppm relative to MPC) via a degassed gastight syringe. Polymerization was performed at 40 °C for 18 h and stopped by immersing the flask in an ice bath and opening it to atmosphere. The product was purified by dialysis against methanol and nanopure water and recovered by lyophilization. The degree of polymerization of PMPC blocks was varied by changing the MPC monomer amount in the reaction.

Synthesis of Br-PPO_{48}-Br Macroinitiator. Poly(propylene oxide) (PPO, M_n ∼ 2700 g/mol) was dissolved in anhydrous toluene and distilled at 90 °C and 100 mTorr for 1 h to remove residual water. The flask was submerged in an ice bath with 4 mol equiv of trimethylamine, followed by dropwise addition of 4 mol equiv of 2-bromoisobutyryl bromide. The reaction was run for 24 h at 20 °C, after which time the mixture was filtered to remove the insoluble hydrobromide salts. After filtration, the reaction mixture was stirred with activated carbon, filtered again, and dried under vacuum. The crude product was mixed with pH 9 water (300 mL) and extracted several times with dichloromethane. The organic layer was further backwashed with 0.5 M sodium bicarbonate, brine (5 M NaCl), and water and then dried with $MgSO_4$ to remove traces of water. The organic mixture was then filtered to remove $MgSO_4$ and dried under vacuum. The degree of esterification was calculated to be 100% based on the disappearance of the hydroxyl peak at 4.41 ppm. Example NMR is shown in Figure S4A.

Polymer Characterization. ^{1}H NMR spectra were recorded on a Bruker AV 400 MHz spectrometer in either DMSO-d_6 or methanol-d_4. Spectra were referenced to DMSO (2.50 ppm) or CD_3OD (3.31 ppm). A representative example of the ^{1}H NMR is provided in Figure S4B for $PMPC_{57}$–PPO_{48}–$PMPC_{57}$. The degree of polymerization (DP) of the purified product was calculated by comparing the signals from the PMPC side chains (δ 4.45–3.86 ppm) and methyl peaks of PPO and PMPC (δ 1.23–0.72 ppm), taking into account that the number of hydrogens corresponding to PPO is 144H.

Static light scattering (SLS) was performed with DAWN HELEOS II (Wyatt Technology) with 120 mW GaAs linearly polarized laser operated at 658 nm. Polymer solutions were dissolved in trifluoroethanol at concentrations ranging from 0.05 to 2.5 mg/mL and were filtered through 0.45 μm PVDF syringe filters (Genesee Scientific) prior to measurements. Pump velocity and flow cell temperature were kept at 0.2 mL/min and 25 °C, respectively. Methoxypoly(ethylene glycol) (5 kDa, Sigma-Aldrich; 5 mg/mL solution in trifluoroethanol) was used as a normalization standard, with R_g set to 2 nm. Values of dn/dc were measured using differential refractometry (see the Supporting Information) and used to determine polymer absolute molecular weight. M_w and second virial coefficient (A_2) values were extracted from Zimm plots using the Astra 6.1 software and the Debye model. Example SLS measurements are shown in Figure S1. Measured NMR and SLS characterization parameters are reported in Table S1.

Polymer-Coated Colloids and Slides. Microscope slides (Fisher 12-549-3) were cleaned before use as described previously[44] and dried with N_2. Clean slides were rendered hydrophobic by spin-coating (3000 rpm, 1 min) with a 3% w/w solution of polystyrene (Sigma-Aldrich 430102) in toluene (Fisher T324). Silica colloids of nominal 1.6–5.0 μm diameter (Bangs Laboratories) were rendered hydrophobic by coating with octadecyl molecules via reaction with octadecanol (Sigma-Aldrich CAS 112-92-5) as described previously.[44] 120 and 400 nm nominal diameter polystyrene sulfate latex (Thermo Fisher Invitrogen S37391) was used as received. Adsorbed polymer layers were formed by dissolving PEO and PMPC copolymers in DI at 0.5–1 mg/mL (above the CMC of 0.01–0.05 mg/mL for all polymers) and contacting polymer solutions with hydrophobic colloids or hydrophobic slides for a minimum of 4 h. Free polymer was removed from particles and slides via centrifugation (particles) and washing (slides) with phosphate buffered saline.

RESULTS AND DISCUSSION

Copolymer Synthesis, Adsorption, Stabilization. To measure interactions of adsorbed PEO–PPO–PEO and PMPC–PPO–PMPC triblock copolymers, we first synthesized and characterized polymers before adsorbing them to particles and surfaces. PMPC–PPO–PMPC triblock copolymers (hereafter termed PMPC copolymers) were synthesized by ARGET-ATRP polymerization (details in the Supporting Information). In brief, PPO_{48} macroinitiator (Figure 1a) was functionalized with 2-bromoisobutyryl bromide and used for atom transfer radical polymerization. Stoichiometric control of reagents was used to vary the degree of polymerization, n, of each PMPC block between n = 10–80, which was characterized by NMR (Figure S1). PMPC copolymer polydispersities were found to have M_w/M_n = 1.1–1.4 from static light scattering (Figure S2 and Table S1). For comparison with PMPC copolymers, commercial PEO–PPO–PEO copolymers (hereafter termed PEO copolymers) were obtained with a range of PEO and PPO repeat unit configurations summarized in Table S2. The PEO blocks vary from n = 17–141, and the PPO blocks vary from n = 29–65. PEO copolymer polydispersities were found to have M_w/M_n = 1.1–1.2 from the literature studies.[26]

To stabilize colloidal particles against aggregation/deposition in physiological ionic strength media (i.e., phosphate-buffered saline, 150 mM NaCl), PMPC and PEO copolymers were adsorbed to silica colloids and glass microscope slides. The silica colloids and glass slide surface were rendered hydrophobic through modifications with octadecyl chains, which has been shown to be necessary to form brush architectures (Figure 1b) for PEO copolymers.[10,26,39,45,46] Silica colloids of diameter 2a = 100–400 nm were stabilized against aggregation using copolymers with PEO blocks with $n \geq 62$ and PMPC blocks with $n \geq 28$ (Figure S4). Likewise, silica colloids of diameter 2a = 1.6–4.8 μm were stabilized against deposition using copolymers with PEO blocks with $n > 76$ and PMPC blocks with $n > 28$ (Figure S5). These results are consistent with expectations in that smaller colloids (with shorter range van der Waals attraction) and higher molecular weight PEO and PMPC blocks (with longer range repulsion) result in the greatest stability. However, the surprising result is that PEO blocks must have 2–3 times as many repeat units as PMPC blocks to impart the same degree of stability. This suggests important differences in layer architectures that we aim to understand via direct measurements of interactions.

Interaction Potentials between Adsorbed Copolymers. Interaction potentials with nanometer and kT-scale resolution were directly measured between colloids and planar surfaces with adsorbed PEO and PMPC copolymers using ensemble TIRM (see the Supporting Information for details).[43,47] Measured ensemble averaged potentials for copolymer coated silica colloids (2a = 2.8 μm) are reported for varying PEO block repeat units (n = 27–141) in Figure 2a and varying PMPC block repeat units (n = 28–80) in Figure 2b. Single particle potentials are similar to each other and the ensemble average interaction (Figure S6) indicating the uniformity of the adsorbed layers on particles and microscope slide, consistent with previous ensemble TIRM measurements.[48,49] For both copolymers, decreasing n decreases the range of repulsion between adsorbed polymer layers. As a result, the net potential varies from purely repulsive to having an attractive well due to van der Waals attraction between the silica particles and glass microscope slides. The PEO

DOI: 10.1021/acs.macromol.8b01792
Macromolecules 2018, 51, 9156–9164

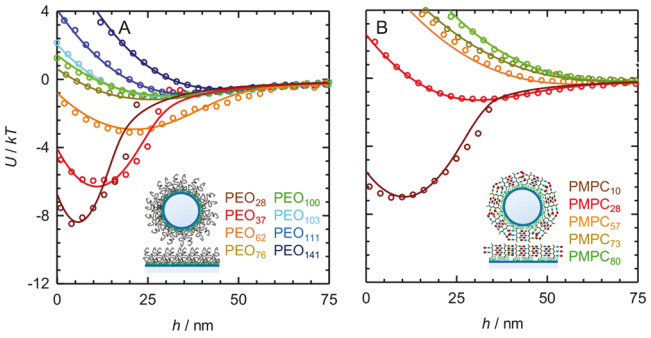

Figure 2. Potential energy profiles (energy vs separation) for molecular weight series of PEO and PMPC copolymers adsorbed to hydrophobic colloids and surfaces. Ensemble total internal reflection microscopy (TIRM) measurements in physiological ionic strength media of 3.2 μm silica colloids and glass surfaces hydrophobically modified with octadecyl chains and adsorbed copolymers of (A) PEO−PPO−PEO with number of PEO repeat units reported in the legend (and PPO repeat units reported in Table S2) and (B) PMPC−PPO−PMPC with the number of PMPC repeat units reported in the legend (and n = 48 for all PPO blocks). Points are ensemble averages of single particle measurements, and lines are given by eq 1 using parameters reported in the text and Supporting Information.

copolymer results also show that varying PPO block sizes appear to have no role (e.g., overlap of PEO_{103}−PPO_{39}−PEO_{103} and PEO_{100}−PPO_{65}−PEO_{100} profiles).

To model the measured interaction potentials, the net potential is considered as the superposition of van der Waals and adsorbed polymer interactions as

$$U(h, a, f_0, L_0) = U_{vdW}(h, a) + U_P(h, a, f_0, L_0) \quad (1)$$

$$U_{vdW}(h, a) = 2\pi a \int_h^\infty \frac{-A_{132}(l)}{12\pi l^2}\, dl \cong -Aah^{-2} \quad (2)$$

$$U_P(h, a, f_0, L_0) = 2\pi a \int_h^{2L_0} 2[f(l/2, L_0) - f_0]\, dl \cong 4\pi a f_0 L_0 \frac{\alpha}{\beta} \exp[-(h\beta/2L_0)] \quad (3)$$

where $A_{132}(l)$ is the Hamaker function for silica and polystyrene interacting across water,[50] f_0 and L_0 are the uncompressed layer free energy per area and layer thickness,[51] and α and β are semiempirical constants[52] (details of derivations and fit parameter in the Supporting Information). Equation 1 does not include electrostatic interactions because the <1 nm Debye length, low zeta potentials (Table S5), and neutral polymers do not yield electrostatic interactions that would contribute significantly to the net superposition of potentials. Equation 2 does not consider contributions to van der Waals attraction from surface roughness or the adsorbed polymer, which have been shown to effectively cancel each other in good solvent conditions for PEO−PPO−PEO[39,53] (although the polymer contribution becomes significant for diminishing solvent quality[41,42,48,54]). The polymer interaction potential (eq 3) was originally developed for flexible polymers with short-range monomer−solvent interactions and should be suitable for PEO[55] (but less so for PMPC layers; this is explored in the following sections). Because the values a and $A(l)$ are known independently, and f_0 approaches a near hard-wall limit on the kT-scale of our measurements, L_0 is the only adjustable parameter. The theoretical fits in Figure 2 using eqs 1−3 accurately capture the net potentials and the adsorbed layer thicknesses vs molecular weight.

Interaction potentials for fixed copolymer molecular weight and varying colloid radius were also directly measured (Figure 3). By varying colloid radius for a fixed copolymer molecular

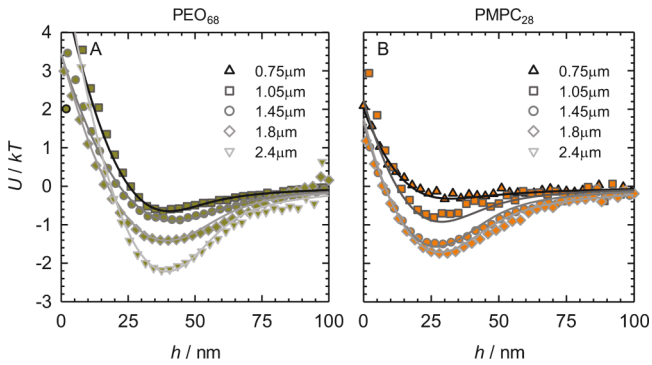

Figure 3. Potential energy profiles (energy vs separation) for fixed molecular weights of adsorbed PEO and PMPC copolymers and different sized colloids (inset legends are colloid radii). Interaction potentials measured for same conditions as Figure 2 but for silica colloid radii and adsorbed layers of (A) PEO_{76}−PPO_{29}−PEO_{76} and (B) $PMPC_{28}$−PPO_{49}−$PMPC_{28}$. Points are ensemble averages of single particle measurements, and lines are given by eq 1 using parameters reported in the text and Supporting Information.

weight, one can use the well-established size-dependent silica van der Waals potential[50] as a "ruler" to measure layer thickness. Using five different silica colloid sizes with radii from a = 0.75−2.4 μm, measured potentials are reported for adsorbed copolymers having PEO blocks with n = 76 (Figure 3a) and PMPC blocks with n = 28 (Figure 3b). These copolymers have similar thicknesses for the same colloid size in Figure 2 and now show nearly similar potentials for different colloid sizes in Figure 3. The potential minimum location is approximately independent of colloid radius, consistent with the Derjaguin approximation and potentials in eqs 2 and 3.[56] In the following sections, we further analyze the potentials in Figures 2 and 3 to estimate how layer thicknesses scale with number of repeat units for both copolymers.

Adsorbed Copolymer Thickness. Here, we analyze the potentials in Figures 2 and 3 to estimate how the uncompressed layer thickness, L_0, scales with number of repeat units, n, for both PMPC and PEO copolymers. Plots in Figure 4 show as points L_0 values obtained from fits to the potentials in Figures 2 and 3 vs repeat unit number for each PEO (Figure 4a) and PMPC (Figure 4b) block. Points are also shown for each adsorbed copolymer's hydrodynamic thickness (from dynamic light scattering[57]) and effective mechanical film thickness (from quart crystal microbalance). A series of lines are also reported in Figure 4, including (1) the radius of gyration, $(n_K/6)^{0.5}L_K$, (2) the number-average molecular weight contour length, $nL_M = (M_n/M_m)L_M$, (3) the weight-average molecular weight contour length, $nL_M = (M_w/M_m)L_M$, (4) a theoretical thickness shown only for PEO (eq S12), and (5) a fit L_0 constrained to the form $L_0 = c1n^{c2}$ ($c1$ and $c2$ reported in the Supporting Information, form chosen based on eq S17).

All thicknesses increase with increasing n, as expected. For both copolymers, the thickness for a given number of repeat units inferred from measured interactions is greater than other measures. This can be expected as the onset of repulsion

DOI: 10.1021/acs.macromol.8b01792
Macromolecules 2018, 51, 9156−9164

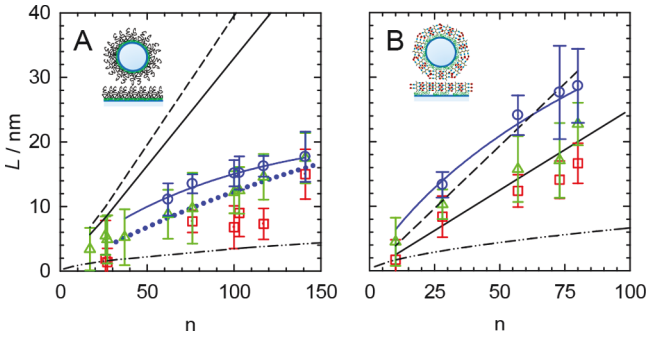

Figure 4. Layer thicknesses vs block repeat units from measurements and model fits for PEO and PMPC copolymers adsorbed to hydrophobic substrates. Measurements are reported as points for (A) PEO and (B) PMPC copolymers from (blue circles) uncompressed layer thicknesses from fits to TIRM measurements in Figures 2 and 3, (green triangles) hydrodynamic thicknesses from DLS measurements, and (red squares) film thicknesses from QCMD. Models and reference dimensions are reported as lines for (blue line) power law fit ($c1n^{c2}$), (dotted blue line) polymer brush theory eq S15, and end block (black dash-dot) radius of gyration ($(n_K/6)^{0.5}L_K$), (black solid) contour length ($(M_n/M_m)L_M$), and (black dashed) weight-averaged molecular weight contour length ($(M_w/M_m)L_M$).

between layers may depend more on chains at the adsorbed layer periphery than measurements of layer hydrodynamics or thin-film mechanics.[6,39] When comparing PEO and PMPC copolymer layers at a given number of repeat units, the PMPC layers thicknesses are 2−3 times greater than the PEO layer thicknesses. This indicates clear differences between the two adsorbed triblock layer architectures.

Various reference polymer dimensions plotted as lines in Figure 4 can be used to understand differences between PEO and PMPC copolymer layer thicknesses and architectures. For the PEO copolymers, the layer thickness falls well within the range bound by the radius of gyration and contour length and is quite close to predictions (eq S15) with no adjustable parameters. In contrast, PMPC layers are highly extended, with the hydrodynamic thicknesses near the number-average molecular weight contour length and the thicknesses from potential energy fits very close to the weight-average molecular weight contour length. Such high PMPC chain extensions are observed in neutron scattering studies[58,59] and simulations of semiflexible brushes when the Kuhn length approaches the contour length[60,61] (which may correspond to the PMPC conditions here). PMPC polydispersity ($M_w/M_n \approx 1.1-1.4$; see the Supporting Information) can also be expected to influence layer thickness.[62,63] Such polydispersity effects are not obvious for PEO layers, however, due to their moderate chain extension and lower polydispersities ($M_w/M_n \approx 1.1-1.2$; see the Supporting Information). The authors are unaware of previous measurements or models of adsorbed copolymer interactions of varying Kuhn length and polydispersity that observe trends similar to Figures 44 (particularly adsorbed polymer layer interactions approaching the weight-averaged molecular weight contour length).

Other mechanisms could lead to thicker than expected PMPC layers, which we address here for completeness, but consider unlikely for cited reasons. For example, surface roughness can influence the range of van der Waals interactions,[50,64] and hence estimates of adsorbed layer thickness from fits to measured potential energy profiles; however, this has been shown not to be the case for adsorbed PEO copolymers in both the present work and previous studies.[39,57] Adsorption is performed above the copolymer critical micelle concentrations (at 1 mg/mL; C_{cmc} between 1 and 50 μg/mL all copolymers) such that micelles could adsorb; however, layers are much thinner (5−30 nm) than micelle dimensions (50−200 nm), and micelle extrusion through 80 nm pore membranes did not change measured interactions (see the Supporting Information). Finally, multilayer or sequential adsorption is unlikely as shown in prior studies of zwitterionic polymers[65,66] and based on the observation of repulsive interactions between adjacent PMPC layers in the present work.

Energy Minima vs Colloid and Polymer Dimensions. To better quantify how net attraction depends on layer and particle properties, Figure 5 summarizes how the potential energy minimum depth, U_M/kT, scales with both particle size and PEO and PMPC copolymer molecular weights. In

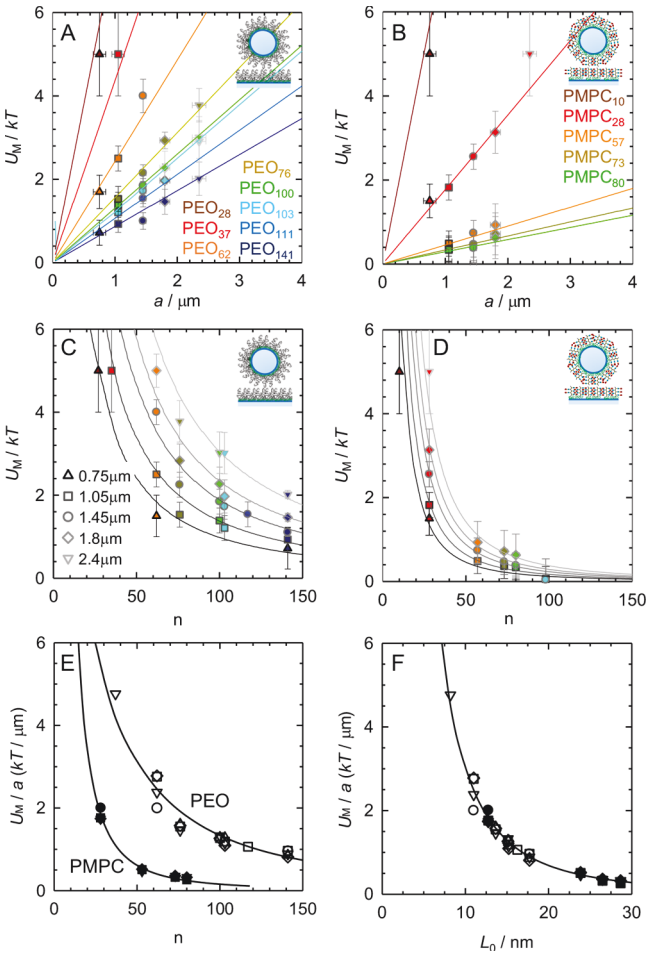

Figure 5. Attractive potential energy minimum well depth vs colloid size and PEO and PMPC block repeat units. Points from measurements in Figures 2 and 3 and lines from eq 1 for potential energy minimum well depth, U_M/kT, vs colloid radius, a, for (A) PEO copolymers and (B) PMPC copolymers and vs block repeat units, n, for (C) PEO copolymers and (D) PMPC copolymers (inset legend is colloid radii). Error bars are 95% confidence intervals from fits. Dividing U_M/kT by a produces (E) two unique curves for (hollow points) PEO and (filled points) PMPC trends vs n and (F) a single universal curve when plotted against the uncompressed layer thickness, which shows equivalence of PEO and PMPC adsorbed copolymer repulsion for same layer thickness.

DOI: 10.1021/acs.macromol.8b01792
Macromolecules 2018, 51, 9156−9164

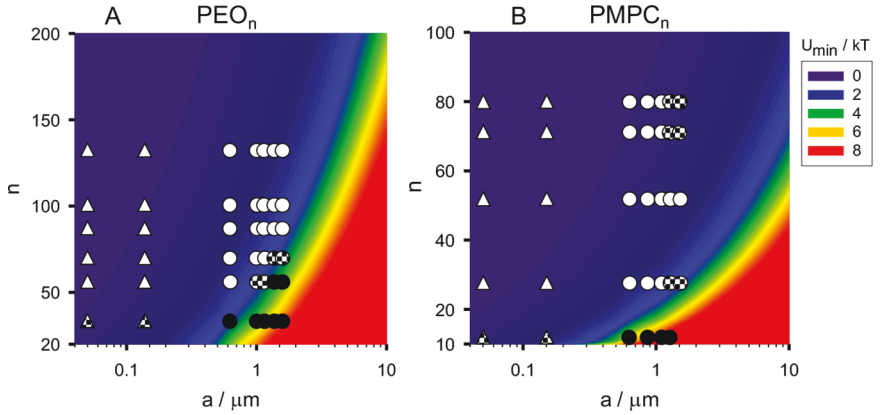

Figure 6. Aggregation and deposition data for PEO and PMPC coated colloids compared to model for energy minimum vs particle radius and number of block repeat units. Data reported for (A) PEO and (B) PMPC copolymers using symbol shape to indicate (triangles) DLS aggregation measurements and (circles) TIRM deposition measurements[68] and symbol fill patterns to indicate (white) stable, (hatch) slow aggregation or deposition, and (black) rapid aggregation or deposition. $U_M(a,n)/kT$ obtained from eq 1 to show how attraction correlates with colloidal stability.

particular, U_M/kT is reported for PEO and PMPC copolymers vs colloid radius (Figure 5a,b) and number of repeat units (Figure 5c,d). Points are obtained from U_M/kT values fit to the measured potential energy profiles in Figures 2 and 3. Lines were plotted by numerically determining $U_M(a)/kT$ and $U_M(n)/kT$ from eq 1 using the fit L_0 curves reported in Figure 4 (with no other adjustable parameters; see the Supporting Information).

As seen in Figure 5a,b, the measured U_M/kT points for both PEO and PMPC layers are linear with a and well captured by eq 1, which is linear in a via the Derjaguin approximation. Increasing n results in a decrease in the slope of U_M/kT versus a in Figures 5a,b for both PEO and PMPC brushes. This n dependence is also accurately captured by eq 1 in the slopes in Figure 5a,b as well as the lines in Figure 5c,d. When comparing the PEO and PMPC results in Figure 5c,d, it is clear that less attraction is observed for the same colloid radius and number of repeat units of PMPC compared to PEO stabilized colloids. For example, for the same number of repeat units with $n \approx 60$ and the same particle diameter with $a = 1.05$ μm, the PMPC-coated particle experiences $\sim 0.5kT$ attraction, whereas the PEO coated particle experiences $\sim 2.5kT$. For similar repeat units, PMPC thus provides greater repulsion (and colloidal stability) due to its greater relative extension away from the surface. This is again a consequence of the PMPC layers being ~2−3 times thicker than PEO layers with the same number of repeat units.

The effectiveness of the model is further demonstrated in Figures 5e,f, which shows $(U_M/kT)/a$ vs n and $(U_M/kT)/a$ vs L_0. By plotting $(U_M/kT)/a$ vs n in Figure 5e, the data and model from Figures 5c,d collapse onto one curve for PEO copolymer and one curve for PMPC copolymer. Practically, dividing the potentials by the colloid radius effectively removes the particle size dependence of the attractive energy minimum as indicated by eq 1 (i.e., dividing both sides by a), but it does not remove the unique n dependence for the two copolymer types. By plotting $(U_M/kT)/a$ vs L_0 in Figure 5f, all data and models collapse onto a single curve for all particle sizes and PEO and PMPC molecular weights.

Because Figures 5f is effectively a plot of $U_M(n)/kT/_a$ (from Figures 5e) vs $L_0(n)$ (from Figure 4a,b), it shows how the model of the colloidal interactions and the layer dimensions together accurately capture all of the measurements in this work. It should also be noted that $0.8L_0$ accurately captures the hydrodynamic thicknesses from DLS in Figure 4 (and could be used to predict layer thicknesses important for lubrication[33]). This suggests that the curve in Figure 5f could be generated from DLS thicknesses by dividing by 0.8 (when direct measurements of interactions are not possible) and practically suggests that the more easily obtainable DLS thickness with a correction factor can be used for predicting interactions.

The results in Figure 5e,f together show PEO and PMPC copolymers allow different amounts of attraction between colloids for the same number of repeat units, but the two copolymers yield the same level of attraction for the same layer thickness. As a result, differences in the ability of the two copolymers to stabilize colloids are unimportant once the two copolymers are compared for conditions that lead to the same layer thickness. In other words, while the extended PMPC layer architecture appears to produce enhanced stability, in the end it produces the same repulsion as a PEO copolymer layer of the same thickness. The fits using eq 1 in Figures 2−5 accurately capture a diverse set of data in terms of potential energy profiles, uncompressed layer thicknesses, particle sizes, molecular weights, and copolymer compositions. These results are obtained in aqueous 150 mM NaCl but should be similar for a range of ionic strengths since PEO and PMPC solvency do not depend on NaCl concentration.[54,67]

Copolymer Mediated Stability (against Aggregation and Deposition). The ability of adsorbed copolymers to mediate attraction between colloids and surfaces practically determines whether particles aggregate or deposit on surfaces. All of the data in Figures 2−5 show that adsorbed PMPC copolymers generate longer range repulsion than adsorbed PEO copolymers with the same n, which results in less attraction between colloids and surfaces. Figure 5c−e perhaps shows most clearly that for the same n, PMPC copolymers results in less attraction than PEO copolymers. In the following, we report aggregation and deposition behavior of PMPC and PEO colloids in physiological media to unambiguously and quantitatively connect measurements and models of interactions to colloidal stability.

Figure 6 shows points from aggregation (triangles) and deposition (circles) measurements using light scattering and optical microscopy (details in the Supporting Information). Points are filled to indicate either stability or slow or rapid

DOI: 10.1021/acs.macromol.8b01792
Macromolecules 2018, 51, 9156−9164

aggregation/deposition, where "rapid" indicates aggregation/deposition on first contact and "slow" indicates kinetics where multiple collisions are required for aggregation/deposition. To connect the deposition behavior to the measured and modeled interactions, contour plots are also shown in Figure 6 for $U_M(a,n)/kT$ from eq 1. There is a clear correspondence between a transition in the data from stable to unstable in the vicinity of the energy contours where $U_M(a,n)/kT \approx 4kT$. The measured interaction potentials and model fit in eq 1 provide quantitative guidance for predicting deposition and aggregation behavior across a wide range PEO and PMPC copolymer molecular weights as well as colloidal particle radii.

Several points in Figure 6 are not well captured by the underlying model for attraction, which tend to occur in limiting cases of molecular weight and particle size. Copolymers having PEO blocks with $n < 28$ and PMPC blocks with $n < 10$ on colloids with $a < 200$ nm exhibit slow aggregation when the model predicts little to no attraction. This discrepancy could arise from extrapolation of modeled interactions that correspond to measurements of larger a and n. Several mechanisms that could lead to lower stability for small a and n include (1) lower adsorbed amounts (see Table S2) that lead to thinner than expected layers, (2) particle curvature reducing lateral crowding to produce thinner layers (for $L_0/a > 0.1$), which would be significant for lower n,[56] and (3) the Derjaguin approximation becomes less valid for scaling potentials for small a.[56,69] Slow deposition was also observed for PMPC copolymers with $n > 73$ when adsorbed to colloids with $a > 1$ μm. Because these particles were stable in the presence of 20 ppm free solution copolymer (Figures S4 and S5), and QCMD measurements indicated partial desorption for these higher molecular weight PMPC copolymers (Figure S9), it seems likely that PMPC desorption destabilized these particles. Smaller particles with the same adsorbed polymers are likely more tolerant of some desorption given their shorter range van der Waals attraction.

Finally, when comparing the PEO and PMPC copolymer stabilization results in Figure 6, the behaviors are practically identical (as in Figure 5f) when PEO copolymers are compared to PMPC copolymers with half as many repeat units, which produces the same layer thicknesses. Although PMPC copolymers can desorb for high molecular weights, a small bulk concentration appears to suppress desorption and stability issues. Given the similar performance of PEO and PMPC copolymers at stabilizing colloids in physiological ionic strength media, it is not clear that one polymer is inherently better than the other one. Future work is in progress to test other performance criteria for PEO and PMPC triblock copolymers including stability in the presence of solution additives, temperature changes, and interactions with various biomaterials.

CONCLUSION

We reported the synthesis of a series of novel PMPC triblock copolymers and compare their interactions and colloidal stabilization performance to PEO triblock analogues. Adsorption of both copolymers to hydrophobic colloids and surfaces produces thick layers that stabilize colloids against aggregation and deposition in physiological ionic strength media. Direct measurements of interaction potentials vs colloid size and copolymer molecular weight, in conjunction with a theoretical model, provide a sensitive measure of adsorbed copolymer layer thickness vs number of block repeat units. This model also captures aggregation/deposition behavior vs particle size, block molecular weight, and copolymer compositions.

Adsorbed PMPC copolymers were found to produce extended architectures with layer thicknesses comparable to PMPC block contour lengths. For the same number of block repeat units, PMPC layers were ~2−3 times thicker than adsorbed PEO copolymer layers, which had thicknesses well described by standard polymer brush theory. However, adsorbed PEO copolymer layers with the same thickness as PMPC layers produced the same repulsion and degree of stability. Our results provide a rigorous explanation for some observations of enhanced PMPC stabilization via extended layers; however, our findings also show that when PEO and PMPC layers of the same thickness are compared, their performance is identical. Understanding symmetric PEO and PMPC interactions in this work provides a basis in future studies to understand their asymmetric interactions with biomaterials for antifouling applications. Ultimately, we report the successful design and synthesis of a novel PMPC triblock copolymer, which we show performs as well as analogous PEO copolymers for stabilizing nano- and microcolloidal particles in physiological media for biomedical applications.

ASSOCIATED CONTENT

Supporting Information

The Supporting Information is available free of charge on the ACS Publications website at DOI: 10.1021/acs.macromol.8b01792.

Additional materials, methods, analysis, and modeling (PDF)

AUTHOR INFORMATION

Corresponding Authors

*E-mail: m.herrera-alonso@colostate.edu.
*E-mail: mabevan@jhu.edu.

ORCID

Margarita Herrera-Alonso: 0000-0002-6064-8699
Michael A. Bevan: 0000-0002-9368-4899

Notes

The authors declare no competing financial interest.

ACKNOWLEDGMENTS

We acknowledge financial support by the National Science Foundation (DMR-171067 and CMMI-1562639) and assistance with QCMD measurements by Kai Loon Chen and Xitong Liu.

REFERENCES

(1) Xing, C. M.; Meng, F. N.; Quan, M.; Ding, K.; Dang, Y.; Gong, Y. K. Quantitative Fabrication, Performance Optimization and Comparison of Peg and Zwitterionic Polymer Antifouling Coatings. *Acta Biomater.* **2017**, *59*, 129−138.

(2) Baba, A.; Taranekar, P.; Ponnapati, R. R.; Knoll, W.; Advincula, R. C. Electrochemical Surface Plasmon Resonance and Waveguide-Enhanced Glucose Biosensing with N-Alkylaminated Polypyrrole/Glucose Oxidase Multilayers. *ACS Appl. Mater. Interfaces* **2010**, *2*, 2347−2354.

(3) Lai, S. K.; O'Hanlon, D. E.; Harrold, S.; Man, S. T.; Wang, Y.-Y.; Cone, R.; Hanes, J. Rapid Transport of Large Polymeric Nanoparticles in Fresh Undiluted Human Mucus. *Proc. Natl. Acad. Sci. U. S. A.* **2007**, *104*, 1482−7.

DOI: 10.1021/acs.macromol.8b01792
Macromolecules 2018, 51, 9156−9164

(4) He, M.; Gao, K.; Zhou, L.; Jiao, Z.; Wu, M.; Cao, J.; You, X.; Cai, Z.; Su, Y.; Jiang, Z. Zwitterionic Materials for Antifouling Membrane Surface Construction. *Acta Biomater.* **2016**, *40*, 142−152.
(5) Russel, W. B.; Saville, D. A.; Schowalter, W. R. *Colloidal Dispersions*; Cambridge University Press: New York, 1989.
(6) Milner, S. T. Polymer Brushes. *Science* **1991**, *251*, 905−914.
(7) Zhao, B.; Brittain, W. J. Polymer Brushes: Surface-Immobilized Macromolecules. *Prog. Polym. Sci.* **2000**, *25*, 677−710.
(8) Halperin, A. Polymer Brushes That Resist Adsorption of Model Proteins: Design Parameters. *Langmuir* **1999**, *15*, 2525−2533.
(9) Tria, M. C. R.; Grande, C. D. T.; Ponnapati, R. R.; Advincula, R. C. Electrochemical Deposition and Surface-Initiated Raft Polymerization: Protein and Cell-Resistant Ppegmema Polymer Brushes. *Biomacromolecules* **2010**, *11*, 3422−3431.
(10) Yasin, S.; Luckham, P. F. Investigating the Effectiveness of Peo/Ppo Based Copolymers as Dispersing Agents for Graphitic Carbon Black Aqueous Dispersions. *Colloids Surf., A* **2012**, *404*, 25−35.
(11) Kostarelos, K.; Tadros, T. F.; Luckham, P. F. Physical Conjugation of (Tri-) Block Copolymers to Liposomes toward the Construction of Sterically Stabilized Vesicle Systems. *Langmuir* **1999**, *15*, 369−376.
(12) Otsuka, H.; Nagasaki, Y.; Kataoka, K. Pegylated Nanoparticles for Biological and Pharmaceutical Applications. *Adv. Drug Delivery Rev.* **2003**, *55*, 403−419.
(13) Jiang, S. Molecular Understanding and Design of Zwitterionic Materials. *Chem. Eng.* **2010**, *920*, 5539.
(14) Schlenoff, J. B. Zwitteration: Coating Surfaces with Zwitterionic Functionality to Reduce Nonspecific Adsorption. *Langmuir* **2014**, *30*, 9625−9636.
(15) Alswieleh, A. M.; Cheng, N.; Canton, I.; Ustbas, B.; Xue, X.; Ladmiral, V.; Xia, S.; Ducker, R. E.; El Zubir, O.; Cartron, M. L.; Hunter, C. N.; Leggett, G. J.; Armes, S. P. Zwitterionic Poly(Amino Acid Methacrylate) Brushes. *J. Am. Chem. Soc.* **2014**, *136*, 9404−9413.
(16) Yang, W.; Zhang, L.; Wang, S.; White, A. D.; Jiang, S. Functionalizable and Ultra Stable Nanoparticles Coated with Zwitterionic Poly(Carboxybetaine) in Undiluted Blood Serum. *Biomaterials* **2009**, *30*, 5617−5621.
(17) Yang, W.; Liu, S.; Bai, T.; Keefe, A. J.; Zhang, L.; Ella-Menye, J. R.; Li, Y.; Jiang, S. Poly(Carboxybetaine) Nanomaterials Enable Long Circulation and Prevent Polymer-Specific Antibody Production. *Nano Today* **2014**, *9*, 10−16.
(18) Leng, C.; Han, X.; Shao, Q.; Zhu, Y.; Li, Y.; Jiang, S.; Chen, Z. In Situ Probing of the Surface Hydration of Zwitterionic Polymer Brushes: Structural and Environmental Effects. *J. Phys. Chem. C* **2014**, *118*, 15840−15845.
(19) Liu, P.; Chen, Q.; Li, L.; Lin, S.; Shen, J. Anti-Biofouling Ability and Cytocompatibility of the Zwitterionic Brushes-Modified Cellulose Membrane. *J. Mater. Chem. B* **2014**, *2*, 7222−7231.
(20) Rajabzadeh, S.; Sano, R.; Ishigami, T.; Kakihana, Y.; Ohmukai, Y.; Matsuyama, H. Preparation of Hydrophilic Vinyl Chloride Copolymer Hollow Fiber Membranes with Antifouling Properties. *Appl. Surf. Sci.* **2015**, *324*, 718−724.
(21) Robinson, K. J.; Coffey, J. W.; Muller, D. A.; Young, P. R.; Kendall, M. A. F.; Thurecht, K. J.; Grøndahl, L.; Corrie, S. R. Comparison between Polyethylene Glycol and Zwitterionic Polymers as Antifouling Coatings on Wearable Devices for Selective Antigen Capture from Biological Tissue. *Biointerphases* **2015**, *10*, 04A305.
(22) Shi, S.; Huang, Y.; Chen, X.; Weng, J.; Zheng, N. Optimization of Surface Coating on Small Pd Nanosheets for in Vivo near-Infrared Photothermal Therapy of Tumor. *ACS Appl. Mater. Interfaces* **2015**, *7*, 14369−14375.
(23) Zhou, T.; Qi, H.; Han, L.; Barbash, D.; Li, C. Y. Towards Controlled Polymer Brushes Via a Self-Assembly-Assisted-Grafting-to Approach. *Nat. Commun.* **2016**, *7*, 11119.
(24) Musoke, M.; Luckham, P. F. Solvent Quality Dependent Interactions between Adsorbed Block Copolymers Measured by Afm. *Colloids Surf., A* **2009**, *337*, 1−8.
(25) Boyes, S. G.; Granville, A. M.; Baum, M.; Akgun, B.; Mirous, B. K.; Brittain, W. J. Recent Advances in the Synthesis and Rearrangement of Block Copolymer Brushes. In *Polymer Brushes: Synthesis, Characterization, Applications*; Advincula, R. C., Brittain, W. J., Caster, K. C., Rühe, J., Eds.; Wiley-VCH Verlag GmbH & Co.: KGaA, Weinheim, 2004; pp 151−165.
(26) Baker, J. A.; Berg, J. C. Investigation of the Adsorption Configuration of Poly (Ethylene Oxide) and Its Copolymers with Poly (Propylene Oxide) on Model Polystyrene Latex Dispersions. *Langmuir* **1988**, *4*, 1055−1061.
(27) Doncom, K. E. B.; Willcock, H.; O'Reilly, R. K. The Direct Synthesis of Sulfobetaine-Containing Amphiphilic Block Copolymers and Their Self-Assembly Behavior. *Eur. Polym. J.* **2017**, *87*, 497−507.
(28) Jiménez, Z. A.; Yoshida, R. Temperature Driven Self-Assembly of a Zwitterionic Block Copolymer That Exhibits Triple Thermoresponsivity and Ph Sensitivity. *Macromolecules* **2015**, *48*, 4599−4606.
(29) Mäkinen, L.; Varadharajan, D.; Tenhu, H.; Hietala, S. Triple Hydrophilic Ucst-Lcst Block Copolymers. *Macromolecules* **2016**, *49*, 986−993.
(30) Canning, S. L.; Neal, T. J.; Armes, S. P. Ph-Responsive Schizophrenic Diblock Copolymers Prepared by Polymerization-Induced Self-Assembly. *Macromolecules* **2017**, *50*, 6108−6116.
(31) Kalasin, S.; Letteri, R. A.; Emrick, T.; Santore, M. M. Adsorbed Polyzwitterion Copolymer Layers Designed for Protein Repellency and Interfacial Retention. *Langmuir* **2017**, *33*, 13708−13717.
(32) Dembele, F.; Tasso, M.; Trapiella-Alfonso, L.; Xu, X.; Hanafi, M.; Lequeux, N.; Pons, T. Zwitterionic Silane Copolymer for Ultra-Stable and Bright Biomolecular Probes Based on Fluorescent Quantum Dot Nanoclusters. *ACS Appl. Mater. Interfaces* **2017**, *9*, 18161−18169.
(33) Chen, M.; Briscoe, W. H.; Armes, S. P.; Klein, J. Lubrication at Physiological Pressures by Polyzwitterionic Brushes. *Science* **2009**, *323*, 1698−1701.
(34) Iuster, N.; Tairy, O.; Driver, M. J.; Armes, S. P.; Klein, J. Cross-Linking Highly Lubricious Phosphocholinated Polymer Brushes: Effect on Surface Interactions and Frictional Behavior. *Macromolecules* **2017**, *50*, 7361−7371.
(35) Kobayashi, M.; Terayama, Y.; Hosaka, N.; Kaido, M.; Suzuki, A.; Yamada, N.; Torikai, N.; Ishihara, K.; Takahara, A. Friction Behavior of High-Density Poly(2-Methacryloyloxyethyl Phosphorylcholine) Brush in Aqueous Media. *Soft Matter* **2007**, *3*, 740−746.
(36) Zhang, Z.; Morse, A. J.; Armes, S. P.; Lewis, A. L.; Geoghegan, M.; Leggett, G. J. Nanoscale Contact Mechanics of Biocompatible Polyzwitterionic Brushes. *Langmuir* **2013**, *29*, 10684−10692.
(37) Musoke, M.; Luckham, P. F. Solvent Quality Dependent Interactions between Adsorbed Block Copolymers Measured by Afm. *Colloids Surf., A* **2009**, *337*, 1−8.
(38) Napper, D. H. Steric Stabilization. *J. Colloid Interface Sci.* **1977**, *58*, 390−407.
(39) Bevan, M. A.; Prieve, D. C. Forces and Hydrodynamic Interactions between Polystyrene Surfaces with Adsorbed Peo-Ppo-Peo. *Langmuir* **2000**, *16*, 9274−9281.
(40) Bevan, M. A.; Prieve, D. C. Effect of Physisorbed Polymers on the Interaction of Latex Particles and Their Dispersion Stability. In *Polymers in Particulate Systems: Properties and Applications*; Hackley, V. A., Somasundran, P., Lewis, J. A., Eds.; Marcel Dekker: New York, 2001.
(41) Bevan, M. A.; Petris, S. N.; Chan, D. Y. C. Solvent Quality Dependent Continuum Van Der Waals Attraction and Phase Behavior for Colloids Bearing Nonuniform Adsorbed Polymer Layers. *Langmuir* **2002**, *18*, 7845−7852.
(42) Bevan, M. A.; Scales, P. J. Solvent Quality Dependent Interactions and Phase Behavior of Polystyrene Particles with Physisorbed Peo-Ppo-Peo. *Langmuir* **2002**, *18*, 1474−1484.
(43) Wu, H.-J.; Pangburn, T. O.; Beckham, R. E.; Bevan, M. A. Measurement and Interpretation of Particle−Particle and Particle−Wall Interactions in Levitated Colloidal Ensembles. *Langmuir* **2005**, *21*, 9879−9888.

DOI: 10.1021/acs.macromol.8b01792
Macromolecules 2018, 51, 9156−9164

(44) Eichmann, S. L.; Meric, G.; Swavola, J. C.; Bevan, M. A. Diffusing Colloidal Probes of Protein-Carbohydrate Interactions. *Langmuir* **2013**, *29*, 2299−310.
(45) Brandani, P.; Stroeve, P. Adsorption and Desorption of Peo - Ppo - Peo Triblock Copolymers on a Self-Assembled Hydrophobic Surface. *Macromolecules* **2003**, *36*, 9492−9501.
(46) Shar, J. A.; Obey, T. M.; Cosgrove, T. Adsorption Studies of Polyethers Part 1. Adsorption onto Hydrophobic Surfaces. *Colloids Surf., A* **1998**, *136*, 21−33.
(47) Wu, H.-J.; Bevan, M. A. Direct Measurement of Single and Ensemble Average Particle-Surface Potential Energy Profiles. *Langmuir* **2005**, *21*, 1244−1254.
(48) Fernandes, G. E.; Bevan, M. A. Equivalent Temperature and Specific Ion Effects in Macromolecule Coated Colloid Interactions. *Langmuir* **2007**, *23*, 1500−1506.
(49) Everett, W. N.; Wu, H.-J.; Anekal, S. G.; Sue, H.-J.; Bevan, M. A. Diffusing Colloidal Probes of Protein and Synthetic Macromolecule Interactions. *Biophys. J.* **2007**, *92*, 1005−1013.
(50) Bitter, J. L.; Duncan, G. A.; Beltran-Villegas, D. J.; Fairbrother, D. H.; Bevan, M. A. Anomalous Silica Colloid Stability and Gel Layer Mediated Interactions. *Langmuir* **2013**, *29*, 8835.
(51) Milner, S. T. Compressing Polymer Brushes - a Quantitative Comparison of Theory and Experiment. *Europhys. Lett.* **1988**, *7*, 695−699.
(52) Eichmann, S. L.; Meric, G.; Swavola, J. C.; Bevan, M. A. Diffusing Colloidal Probes of Protein−Carbohydrate Interactions. *Langmuir* **2013**, *29*, 2299−2310.
(53) Dagastine, R. R.; Bevan, M. A.; White, L. R.; Prieve, D. C. Calculation of Van Der Waals Forces with Diffuse Coatings: Applications to Roughness and Adsorbed Polymers. *J. Adhes.* **2004**, *80*, 365−394.
(54) Hwang, K.; Wu, H.-J.; Bevan, M. A. Specific Ion-Dependent Attraction and Phase Behavior of Polymer-Coated Colloids. *Langmuir* **2004**, *20*, 11393−11401.
(55) Milner, S.; Witten, T.; Cates, M. Theory of the Grafted Polymer Brush. *Macromolecules* **1988**, *21*, 2610−2619.
(56) Li, H.; Witten, T. A. Polymers Grafted to Convex Surfaces: A Variational Approach. *Macromolecules* **1994**, *27*, 449−457.
(57) Min, G.; Bevan, M. A.; Prieve, D. C.; Patterson, G. D. Light Scattering Characterization of Polystyrene Latex Spheres with and without Adsorbed Polymer. *Colloids Surf., A* **2002**, *202*, 9−21.
(58) Kobayashi, M.; Ishihara, K.; Takahara, A. Neutron Reflectivity Study of the Swollen Structure of Polyzwitterion and Polyeletrolyte Brushes in Aqueous Solution. *J. Biomater. Sci., Polym. Ed.* **2014**, *25*, 1673−1686.
(59) Matsuda, Y.; Kobayashi, M.; Annaka, M.; Ishihara, K.; Takahara, A. Dimensions of a Free Linear Polymer and Polymer Immobilized on Silica Nanoparticles of a Zwitterionic Polymer in Aqueous Solutions with Various Ionic Strengths. *Langmuir* **2008**, *24*, 8772−8778.
(60) Egorov, S. A.; Hsu, H.-P.; Milchev, A.; Binder, K. Semi Fl Exible Polymer Brushes and the Brush- Mushroom Crossover. *Soft Matter* **2015**, *11*, 2604−2616.
(61) Milchev, A.; Binder, K. Semiflexible Polymers Grafted to a Solid Planar Substrate: Changing the Structure from Polymer Brush to " Polymer Bristle. *J. Chem. Phys.* **2012**, *136*, 194901.
(62) de Vos, W. M.; Leermakers, F. A. M. Modeling the Structure of a Polydisperse Polymer Brush. *Polymer* **2009**, *50*, 305−316.
(63) Milner, S. T.; Witten, T. A.; Cates, M. E. Effects of Polydispersity in the End-Grafted Polymer Brush. *Macromolecules* **1989**, *22*, 853−861.
(64) Bevan, M. A.; Prieve, D. C. Direct Measurement of Retarded Van Der Waals Attraction. *Langmuir* **1999**, *15*, 7925−7936.
(65) Kharlampieva, E.; Izumrudov, V. A.; Sukhishvili, S. A. Electrostatic Layer-by-Layer Self-Assembly of Poly(Carboxybetaine)-S: Role of Zwitterions in Film Growth. *Macromolecules* **2007**, *40*, 3663−3668.
(66) Salloum, D. S.; Olenych, S. G.; Keller, T. C. S.; Schlenoff, J. B. Vascular Smooth Muscle Cells on Polyelectrolyte Multilayers: Hydrophobicity-Directed Adhesion and Growth. *Biomacromolecules* **2005**, *6*, 161−167.
(67) Kobayashi, M.; Terayama, Y.; Kikuchi, M.; Takahara, A. Chain Dimensions and Surface Characterization of Superhydrophilic Polymer Brushes with Zwitterion Side Groups. *Soft Matter* **2013**, *9*, 5138.
(68) Coughlan, A. C. H.; Torres-Diaz, I.; Jerri, H. A.; Bevan, M. A. Direct Measurements of Kt-Scale Capsule−Substrate Interactions and Deposition Versus Surfactants and Polymer Additives. *ACS Appl. Mater. Interfaces* **2018**, *10*, 27444−27453.
(69) Pailthorpe, B. A.; Russel, W. B. The Retarded Van Der Waals Interaction between Spheres. *J. Colloid Interface Sci.* **1982**, *89*, 563−566.

DOI: 10.1021/acs.macromol.8b01792
Macromolecules 2018, 51, 9156−9164